Carbon Nanotube Based High Resolution Holograms

Article *in* Advanced Materials · November 2012

DOI: 10.1002/adma.201202593 · Source: PubMed

8 authors, including:

Haider Butt
Khalifa University
282 PUBLICATIONS **9,272** CITATIONS

SEE PROFILE

Sai Shivareddy
University of Cambridge
9 PUBLICATIONS **225** CITATIONS

SEE PROFILE

Timothy D. Wilkinson
University of Cambridge
329 PUBLICATIONS **6,201** CITATIONS

SEE PROFILE

Carbon Nanotube Based High Resolution Holograms

Haider Butt, Yunuen Montelongo, Tim Butler, Ranjith Rajesekharan, Qing Dai, Sai G. Shiva-Reddy, Timothy D. Wilkinson, and Gehan A. J. Amaratunga*

The advancements in nanofabrication and microscopy techniques have provided us with great control over the fabrication of carbon nanotubes (CNTs),[1] where we can engineer their dimensions, material properties and precise localization.[2] Therefore, in recent years vast numbers of nanophotonic applications have been reported where the interaction of light with engineered CNTs arrays has been utilized to solve different challenges encountered by the optical industry. The examples being the usage of CNTs for optical imaging and sensing,[3] as electrodes in display devices,[4] for producing efficient solar cells,[5] photonic crystals,[6] and metamaterials.[7–9] Similarly one of the challenges faced by the state of the art holographic displays systems and spatial light modulators (SLMs) is the finite size of the pixels used. Pixels in these systems fundamentally represent the smallest optical scattering elements. Light scattered from individual pixels interferes spatially to produce the projected images/diffraction patterns.[10] The pixel size controls both the resolution and field of view of these projected images.[11] Smaller pixels allow the diffraction of light at larger angles increasing the field of view. To address this limitation we propose the utilization of subwavelength nanostructures (CNTs) as diffractive elements to produce high resolution and wide field of view holograms. Here, we used arrays of vertically aligned multiwalled carbon nanotubes (MWCNTs) as pixels to produce binary amplitude holograms, achieving low noise high resolution images with wide field of view.

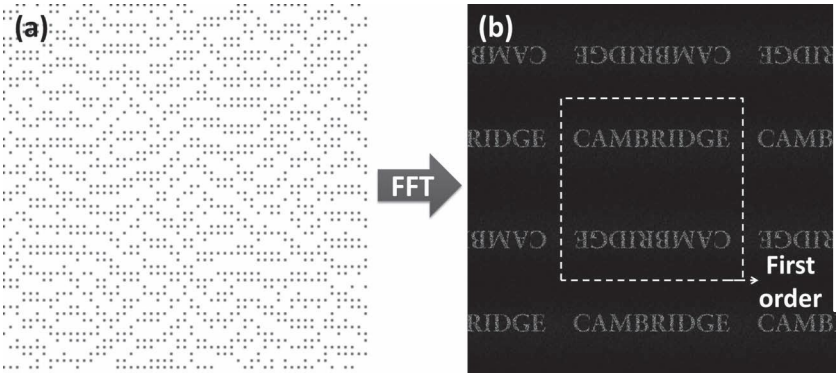

Figure 1. Calculation results for the 2D holographic pattern. a) A cropped image of the calculated 2D hologram based on 300 × 300 square array of multiwalled carbon nanotubes. The array lattice constant is 400 nm. b) 2D Fourier transform of the whole nanotube array producing a diffraction pattern consisting of symmetric CAMBRIDGE images. The zero order was removed from the image.

CNTs in general have been the focus of enormous research during the last decade due to their interesting electrical and optical properties.[12] With well established nanofabrication processes plasma enhanced chemical vapour deposition (PECVD), highly controlled fabrication of vertically aligned CNT arrays can be performed with predetermined dimensions and spatial locations.[13–15] Periodic arrays of CNTs can be fabricated at lattice constants that are comparable to the wavelengths of visible light (few hundred nanometers), giving rise to interesting optical effects such as diffraction.[16] Kempa et al,[6] was the first to report that hexagonal lattice CNT arrays display strong diffraction effects due to the nanoscale array dimensions and the metallic characteristics of CNTs. The far field intensity patterns (and the field of view) were dictated by the spatial locations of CNT in the array.

Our objective was to control the angular diffraction from CNT array by fabricating these arrays in the form of a holographic pattern. The array of subwavelength nanotubes can act as an intensity hologram (grid of apertures) towards the incident light, producing a diffraction pattern (CAMBRIDGE) in the far field. In this manner we can replicate the mechanism of an intensity SLM while using the world's smallest pixel defined by a nanoscaled CNT.

We utilised the principle of Fourier optics[17] to calculate the MWCNT array (hologram) that would produce a CAMBRIDGE image. The array represented a binary intensity mask that would produce a pattern in the far field similarly to a Fraunhofer hologram. In this way the far field can be expressed as the Fourier transform of the mask. The CNT hologram was modeled as a square array of 300 × 300 intensity deltas spaced by a lattice constant of 400 nm and a tube diameter of 80 nm. The binary amplitude array was optimized by using the Gerchberg–Saxton (GS) algorithm.[18] **Figure 1**a shows the optimized solution for the CNT array based hologram.

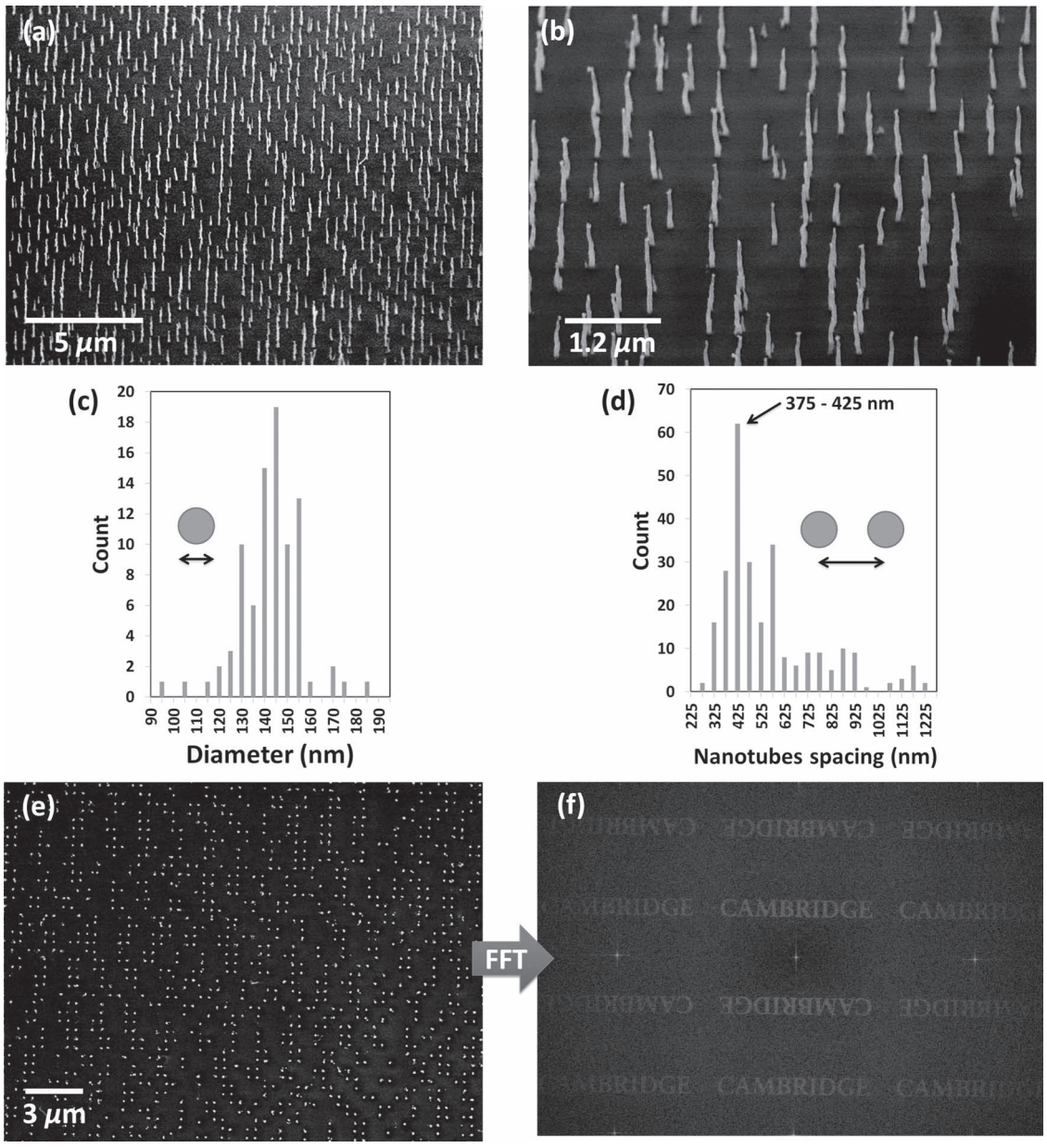

Figure 2. Images of CNT array. a) SEM image of the fabricated MWCNT array taken at 30° from the vertical and (b) a zoomed in version of the same image. c) Histogram showing the diameter distribution in the CNT arrays (average of 140 nm and standard deviation of 13 nm). d) Distribution of periodic spacing between the nanotubes in the hologram. The distances between 375 to 425 nm showed the highest frequency. e) Cropped SEM image of the nanotube array taken from normal angle (perpendicular to the sample). f) 2D FFT of the complete SEM image produces a diffraction pattern with symmetric CAMBRDIGE images.

Figure 1b shows the 2D Fast Fourier Transform (FFT) of the whole CNT hologram. It can be observed that several orders of symmetrical conjugate CAMBRIGDE images were predicted for the hologram. A high intensity zero order located in the centre of the image was removed to view the first and second orders clearly. The calculations were performed based on the principle of diffraction optics assuming the CNTs acted as diffracting elements. The calculations did not take into account the near field optical effects like surface plasmons and nano-antenna resonances, usually attributed to the nanophotonic structures.

Based on the calculated holographic patterns the fabrication of CNT array was performed. The array was fabricated on a 10 × 10 mm silicon (Si) substrate which was first cleaned in acetone and then in isophthalic acid (IPA) followed by spin coating with a 150 nm layer of Polymethyl methacrylate (PMMA). The sample was then patterned using a NanoBeam electron beam lithography system and developed for 70 s in a solution of (metal isobutyl ketone) MIBK:IPA at a ratio of 1:2. A 5 nm barrier layer of indium tin oxide (ITO) followed by 15 nm of nickel catalyst was sputtered in an argon atmosphere at a pressure of

350 Pa. Subsequently lift-off was carried out in acetone, leaving the desired pattern of catalyst dots on the Si substrate.

An optimized PECVD growth recipe, demonstrated in[7] was used for the current nanotube array with a square lattice constant of 400 nm. The nanotubes were grown in a NanoInstruments "Black Magic" PECVD system with acetylene as the feedstock gas and ammonia as the etchant. The plasma was maintained at a voltage of 650 V and a current of 60 mA. A growth time of 15 min at a pressure of ≈300 Pa yielded the MWCNT array with a tube length of approximately 1500 nm in 2.5 mm^2 area. Scanning electron microscrograph (SEM) of the fabricated nanotube array is shown in **Figure 2**a, with a magnified view in Figure 2b. Highly ordered array of vertically aligned MWCNTs was obtained. To characterize the CNT diameter and periodicity distribution of the array, statistical analysis was performed on an SEM taken from normal incident. The grayscale SEM image was converted into a binary black-and-white image. Image processing software was utilized to measure the sizes, shapes, and center positions of the nanotubes from the black-white images. The diameter distribution analysis in Figure 2c shows that the majority of the nanotubes have diameters in the range 135–150 nm, with an average diameter of 140 nm and standard deviation of 13 nm. The distribution of center to center distance between the nearest-neighbor nanotubes was calculated from the positions of nanotube centers. The distribution histogram in Figure 2d shows that the most common center to center distance between the nanotubes was in the range of 375–425 nm. The second prominent peak in the bell-shaped histogram was above the number 575 (interval 525–575), indicating the diagonal next-nearest neighbour distance of $1.414 \times 400 = 566$ nm. This proves that the square periodicity of approximately 400 nm (dictated by the process of electron beam lithography) was the predominant feature of the hologram.

Figure 2e shows a cropped SEM image of the nanotube based hologram taken normal to the substrate. It can be observed that the square lattice consist of 50% of the nanotubes. Using this experimental data (the whole SEM image), a Fourier transform was carried out. The Fourier transform of the SEM CNT array displayed CAMBRIDGE images symmetrically localized around the zero order (Figure 2f). The highly intense zero order consisting of the undiffracted light has been removed from the FFT image to make the CAMBRDIGE images clearer. The results showed that the nanotube array was accurately fabricated and could perform as a binary amplitude intensity hologram towards impinging light to produce CAMBRIDGE image in the far field.

The optical characterization of the nanotube based hologram was performed. The Si substrate bearing the CNT hologram was mounted onto a post with a semitransparent hemispherical screen set above it. The hemispherical screen had a radius of the order of 15 cm which allowed sufficient distance to capture diffraction patterns in the far field. The base of the screen was placed parallel to the plane of the sample and the screen had a small aperture in its center to allow the passage of incident laser, as shown in **Figure 3**a. A 532 nm (green) laser was mounted above the screen, arranged so that the beam was normally incident at the sample. The reflected diffraction pattern produced when the CNT hologram was illuminated was captured by a camera.

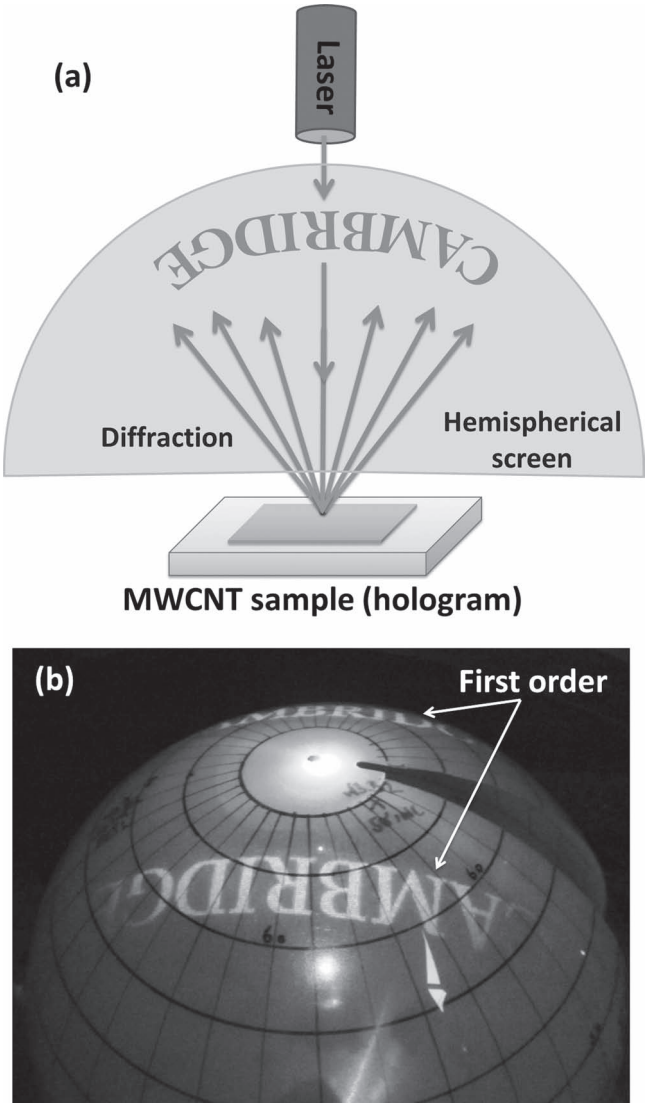

Figure 3. Experimental setup and measured diffraction pattern results. a) The schematic diagram of the experimental setup employed to capture the diffraction pattern. b) The pattern was obtained on a semitransparent hemispherical screen of radius 15 cm by shining a green (532 nm) laser perpendicular to the plane of the CNT array. A clear CAMBRIDGE image was observed in the first order of the diffraction pattern.

Figure 3b shows the observed diffraction pattern which was in excellent agreement with the calculated results. The first order diffraction pattern (replay field) consisted of two symmetrically conjugate CAMBRIDGE images placed on opposite sides of the hemispherical screen. The higher orders diffraction patterns were not observed as they were projected at very large angles (>90 degrees to the normal) due to the nanoscale periodicity of the CNT array. A highly clear and intense CAMBRIDGE image was produced encompassing a wide field of view. This was due to the high resolution CNT array based hologram having around 45 000 pixels (diffracting elements) in a 120 μm^2 area. Due to highly periodic and ordered nanotube array there was negligible noise and unwanted spots in the diffraction pattern, producing very high contrast image.

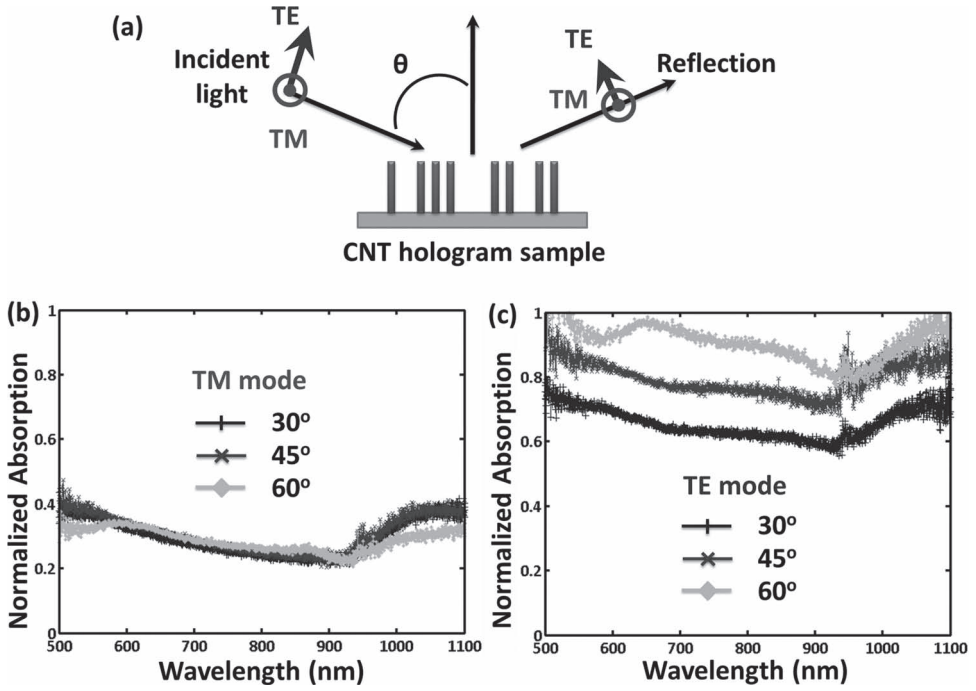

Figure 4. Experimental setup and measured angle dependent absorption spectra. a) Schematic representation of the experimental setup. b,c) The absorption measurement from the sample for light polarized (b) parallel (TE) and (c) perpendicular (TM) to the MWCNTs.

The intense zero order was observed in Figure 3b consisting of the un-diffracted light which did not interact with the CNTs and was mostly reflected from the Si substrate. According to the geometrical calculations, around 98.5% of the incident light should present in the zero order as CNTs occupy only about 1.5% of the total area in the binary amplitude hologram. This can be observed from the SEM image of the fabricated sample (Figure 2c). Under these circumstances the zero order will be bright enough to saturate the camera and the first order CAMBRIGDE images would not be visible. However, as observed in Figure 3b, the CAMBRIDGE diffraction pattern was clearly visible even in the presence of the zero order suggesting the CNT based hologram presents higher diffraction efficiency.

Diffraction efficiency measurements were performed in order to clarify the origin of the unexpected high contrast at the image. The intensity of light in the zero and first order was measured to calculate efficiency. The first order, consisting of CAMBRIDGE image, was measured by placing a high numerical aperture lens near the sample to focus all the diffracted light into the photodiode. Diffraction efficiency of the order of 10% was recorded from the nanotube array at normal incidence, representing an enhancement of the order of 6 times higher than the geometrical calculation. This is due to the high metallic character and large scattering cross-section of MWCNTs[6,16,19] which allows them to act as exceptional optical scattering elements.

Furthermore, in contrast to the conventional two dimensional (2D) holograms, CNT arrays have a 3D structure that causes the optical diffraction in an anisotropic manner.[20] The diffraction from nanotube arrays is expected to be dependent on the angle of incidence and the polarization of light. At normal incidence no considerable polarization dependence was observed in the diffraction efficiency measurements. However, at higher incident angles variation in diffraction and absorption is expected for light polarized parallel and perpendicular to the nanotubes. Kimble[21] had previously demonstrated the angular diffraction efficiency measurement from the CNT arrays. The measurements suggested that nanotubes arrays display higher diffraction efficiency and absorption towards light polarized parallel to the CNTs. With the increase in incident angle the diffraction efficiency increases due to the larger CNT cross-sectional area exposed increasing the overall area covered by the diffractive elements.

To study the polarization dependence of absorbed light, angular absorption measurements were carried out on the CNT array. The CNT hologram was characterized using a spectrometer setup. An Ocean Optics white-light source with an optical spectrum from 450 to 1100 nm was utilized for illumination. Measurements were performed for light polarised parallel (transverse electric (TE) mode) and perpendicular (transverse magnetic (TM) mode) to the nanotubes, as shown in **Figure 4**a. Polarization of the white-light beam was selected before the beam was guided onto the sample. Microscope objectives were used to collimate the light beam coming out of the fibre and to focus it onto the sample. The reflected light was focused back into the fibre by placing a series of lenses and objectives very close to the sample. An Ocean Optics 2000 spectrometer was utilized to capture the reflected signal for the spectral range of almost 500 to 1100 nm, with resolution of 0.2 nm.

The absorption spectra measured at incident angles of 30, 45, and 60 degrees with respect to the vertical are shown in Figure 4b,c. Absorption measurements from the CNT hologram

were done relative to plane silicon substrate. For the light polarized perpendicular (TM) to the nanotubes a consistent absorption was observed with changing incident angles. Only slight increase in absorption was observed with the increase in incident angle from 30 to 60 degrees. As shown in Figure 4b, the normalized TM absorption at $\lambda = 800$ nm increased from 0.23 to 0.26 for incident angles varying from 30 to 60 degrees. For the light polarized parallel (TE) to the nanotubes much higher absorption was observed. For TE mode the CNT cross-sectional area exposed to light increases drastically with increasing incident angles causing higher absorption. The TE mode absorption spectra measurements show that with increasing incident angles the light absorbed by the hologram increased. As shown in Figure 4c, for $\lambda = 800$ nm the normalized TE absorption was of the order of 0.62, 0.74, and 0.90 at incidence angles of 30, 45, and 60 degrees, respectively. The absorption measurements recorded the light reflected from the CNT hologram with reference to the plane silicon substrate. The light not reflected back was either absorbed by the nanotubes or diffracted at large angles into the CAMBRIDGE hologram. The drastic increase in TE absorption with incident angle can suggest that both the absorption in nanotubes and the diffraction is increasing. At higher incident angles light is exposed to a larger area of diffracting elements (nanotubes) which increased the diffraction efficiency. The results are consistent with the diffraction efficiency measurements reported in Ref. [21].

The angular diffraction measurements could not be performed with the current CNT hologram. The incident light was diffracted at large angles forming the CAMBRIDGE image. It was very challenging to capture all the diffracted light into a lens and focus all the wavelengths back into the spectrometer. However, a CNT hologram can be designed in the future which diffracts light into a spot in the far field. Angle dependent spectral diffraction measurements can be easily performed from such holograms.

The wavelength dependence of diffraction from CNT hologram was also studied. The nanoscale dimensions of the CNT array cause the diffraction of light at large angles increasing the field of view. According to the principle of Bragg diffraction the diffraction angle is dependent on wavelength. The diffraction patterns from the CNT hologram was studied under blue (454 nm), green (532 nm) and red (635 nm) lasers. As shown in **Figure 5** with the increase in laser wavelength the CAMBRIDGE image was diffracted at larger angles producing larger images. In response to the red laser, CAMBRIDGE image was diffracted to the largest angle of around 35 degree from the vertical, whilst the green and blue lasers produced the same image at 27 and 23 degree respectively. The effect was in excellent agreement with Bragg's law. Due to the small diffraction angle with the blue laser, a part of second order CAMBRIDGE image was also observed at an angle of 50 degrees (Figure 5a).

Figure 5d shows a zoomed in version of the image where each diffracted red laser spot in the CAMBRDIGE image can be viewed clearly. The diameter of each diffracted spot was approximate 0.4 mm, when viewed on the semitransparent hemispherical screen of radius 15 cm. Such discretization of spots is not observed for the blue and green lasers as the spacing between them is too small. Each spot represents the diffracted light originating from the CNT pixels. According to the calculations, the total number of spots constructing the CAMBRIDGE image was equal to the number of pixels utilized to construct the hologram that is 300 × 300. The resolution of

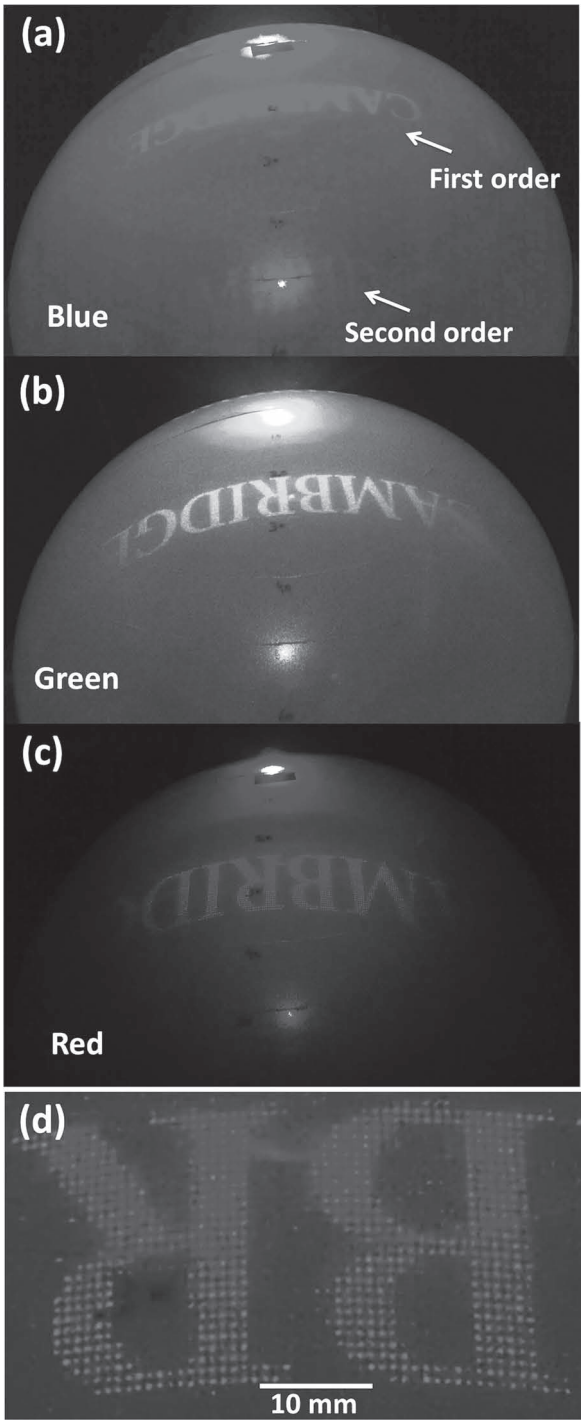

Figure 5. Diffraction patterns from CNT based holograms for different lasers. Diffracted CAMBRIDGE image produced while shining (a) blue (454 nm), (b) green (532 nm) and (c) red (454 nm) laser perpendicular to the plane of the lattice. d) Zoomed in view of the image produced by the red laser. Due to the large diffraction angle each diffracted pixel (of approximate size 0.4 mm) can be discretely viewed.

the diffracted image can be further increased by increasing the size of the CNT based hologram.

In conclusion, we have reported the novel utilization of nanostructures (multiwalled carbon nanotubes) as the smallest diffracting elements ever for producing holograms. Multiwalled carbon nanotubes are well known for their excellent optical scattering capacity and can be fabricated in a highly controlled manner. We report the controlled scattering from carbon nanotubes by patterning their arrays to form high resolution hologram which produce the image of CAMBRIDGE in the far field. Due to the nanoscale dimension of nanotubes the diffraction images produced displayed very large field of view and high contrast. These results pave the way towards utilization of nanostructures for producing 3D holograms with wide field of view and high resolution.

Acknowledgements

This work was partly funded under the Nokia-Cambridge Strategic Partnership in Nanoscience and Nanotechnology (Energy Programme). The authors thank Ananta Palani and Umair Hassan for the fruitful discussions.

Received: June 26, 2012
Revised: July 31, 2012
Published online: August 31, 2012

[1] S. Iijima, *Nature* **1991**, *354*, 56.
[2] M. Meyyappan, D. Lance, C. Alan, H. David, *Plasma Sources Sci. Technol.* **2003**, *12*, 205.
[3] R. Rajasekharan, T. D. Wilkinson, P. J. W. Hands, Q. Dai, *Nano Lett.* **2011**, *11*, 2770.
[4] T. D. Wilkinson, X. Wang, K. B. K. Teo, W. I. Milne, *Adv. Mater.* **2008**, *20*, 363.
[5] H. Zhou, A. Colli, A. Ahnood, Y. Yang, N. Rupesinghe, T. Butler, I. Haneef, P. Hiralal, A. Nathan, G. A. J. Amaratunga, *Adv. Mater.* **2009**, *21*, 3919.
[6] K. Kempa, B. Kimball, J. Rybczynski, Z. P. Huang, P. F. Wu, D. Steeves, M. Sennett, M. Giersig, D. V. G. L. N. Rao, D. L. Carnahan, D. Z. Wang, J. Y. Lao, W. Z. Li, Z. F. Ren, *Nano Lett.* **2002**, *3*, 13.
[7] H. Butt, Q. Dai, R. Rajesekharan, T. D. Wilkinson, G. A. J. Amaratunga, *ACS Nano* **2011**, *5*, 9138.
[8] H. Butt, Q. Dai, P. Farah, T. Butler, T. D. Wilkinson, J. J. Baumberg, G. A. J. Amaratunga, *Appl. Phys. Lett.* **2010**, *97*, 163102.
[9] D. R. Smith, J. B. Pendry, M. C. K. Wiltshire, *Science* **2004**, *305*, 788.
[10] S. Larouche, Y.-J. Tsai, T. Tyler, N. M. Jokerst, D. R. Smith, *Nat. Mater.* **2012**, *11*, 450.
[11] R. Stahl, M. Jayapala, *Opt. Photonik* **2011**, *6*, 39.
[12] P. M. Ajayan, J. M. Tour, *Nature* **2007**, *447*, 1066.
[13] M. Chhowalla, K. B. K. Teo, C. Ducati, N. L. Rupesinghe, G. A. J. Amaratunga, A. C. Ferrari, D. Roy, J. Robertson, W. I. Milne, *J. Appl. Phys.* **2001**, *90*, 5308.
[14] K. B. K. Teo, M. Chhowalla, G. A. J. Amaratunga, W. I. Milne, D. G. Hasko, G. Pirio, P. Legagneux, F. Wyczisk, D. Pribat, *Appl. Phys. Lett.* **2001**, *79*, 1534.
[15] Z. F. Ren, Z. P. Huang, J. W. Xu, J. H. Wang, P. Bush, M. P. Siegal, P. N. Provencio, *Science* **1998**, *282*, 1105.
[16] J. Rybczynski, K. Kempa, Y. Wang, Z. F. Ren, J. B. Carlson, B. R. Kimball, G. Benham, *Appl. Phys. Lett.* **2006**, *88*, 203122.
[17] J. W. Goodman, *Introduction to Fourier Optics*, Roberts and Company Publishers, Englewood, CO, USA **2005**.
[18] R. W. Gerchberg, O. Saxton, *Optik* **1972**, *35*, 237.
[19] P. Wu, B. Kimball, J. Carlson, D. V. G. L. N. Rao, *Phys. Rev. Lett.* **2004**, *93*, 013902.
[20] K. C. Hsieh, T. Y. Tsai, D. H. Wan, H. L. Chen, N. H. Tai, *Carbon* **2012**, *48*, 1410.
[21] B. R. Kimball, J. B. Carlson, D. M. Steeves, K. Kempa, Z. Ren, P. Wu, T. Kempa, G. Benham, Y. Wang, W. Li, A. Herczynski, J. Rybczynski, D. V. Rao, "Diffraction Effects in Honeycomb Arrays of Multiwalled Carbon Nanotubes", presented at *Nanoengineering: Fabrication, Properties, Optics, and Devices*, Denver, CO, USA **2004**.